Global Journal of Medical Research: B
Pharma, Drug Discovery, Toxicology & Medicine
Volume 18 Issue 2 Version 1.0 Year 2018
Type: Double Blind Peer Reviewed International Research Journal
Publisher: Global Journals
Online ISSN: 2249-4618 & Print ISSN: 0975-5888

A DFT-Based QSAR and Molecular Docking Studies on Potent Anti-Colon Cancer Activity of Pyrazole Derivatives

By IBRAHIM, Asiata Omotayo, Abel Kolawole Oyebamiji, Oyeladun Rhoda Oyewole & Banjo Semire

Ladoke Akintola University of Technology

Abstract- Pyrazole derivatives have been described as a group of compounds with various biological activities including anticancer effect. Therefore, a set of twenty Pyrazole based compounds which had been previously shown to be active against human colon cancer cell (HT29) are use in the study. These compounds were optimized using Density Functional Theory (DFT) for the calculations of molecular descriptors that related the bioactivity of these compounds to their structures. The developed quantitative structure activity relation (QSAR) was validated, and it showed the reliability and acceptability of the model. The in silico simulations were carried out on the twenty Pyrazole based compounds with colon cancer cell line, HT29 (PDB ID: 2N8A) using Autodock vina software. The docked complexes were validated and enumerated based on the AutoDock Scoring function to pick out the best inhibitors based on docked Energy. The analysis of the ligand-receptor complexes showed that H-bonds played a prominent role in the binding and posed stability of the ligand in the ligandreceptor complexes. The binding free energy, **Δ**G calculated ranged from - 6.10 kcal/mol – 8.20 Kcal/mol.

Keywords: pyrazole derivatives, DFT-QSAR, molecular docking.

GJMR-B Classification: NLMC Code: QV 4

Strictly as per the compliance and regulations of:

A DFT-Based QSAR and Molecular Docking Studies on Potent Anti-Colon Cancer Activity of Pyrazole Derivatives

IBRAHIM, Asiata Omotayo [α], Abel Kolawole Oyebamiji [σ], Oyeladun Rhoda Oyewole [ρ] & Banjo Semire [ω]

Abstract- Pyrazole derivatives have been described as a group of compounds with various biological activities including anticancer effect. Therefore, a set of twenty Pyrazole based compounds which had been previously shown to be active against human colon cancer cell (HT29) are use in the study. These compounds were optimized using Density Functional Theory (DFT) for the calculations of molecular descriptors that related the bioactivity of these compounds to their structures. The developed quantitative structure activity relation (QSAR) was validated, and it showed the reliability and acceptability of the model. The *in silico* simulations were carried out on the twenty Pyrazole based compounds with colon cancer cell line, HT29 (PDB ID: 2N8A) using Autodock vina software. The docked complexes were validated and enumerated based on the AutoDock Scoring function to pick out the best inhibitors based on docked Energy. The analysis of the ligand-receptor complexes showed that H-bonds played a prominent role in the binding and posed stability of the ligand in the ligand-receptor complexes. The binding free energy, ΔG calculated ranged from - 6.10 kcal/mol – 8.20 Kcal/mol.

Keywords: pyrazole derivatives, DFT-QSAR, molecular docking.

I. Introduction

Cancer is not a contagious neither infectious disease, but it has become a second leading cause of death worldwide and travels from one end to the other via bloodstream within the body system [1,2]. It can be caused by both external and internal factors, e.g. tobacco, infectious organisms, chemicals, and radiation are for outside while inherited mutations, hormones, and immune conditions for internal factor. Moreover, all of these factors may work together or in series to start or enhance carcinogenesis[3]. The cure for cancer remain surgery, chemotherapy and radiation therapy and adult, as well as, children can be affected. However, cases of children having cancer are limited[4].

Colon cancer as a worldwide known health problem forays more than a million people every year, which has been the cause of death to over 600,000 people[5]. It is found to be the usual cause of death in comparison to other types of cancer that exist[6,7]. Several features that may cause an increment in colon cancer risks comprise diet, diabetes, aging, obesity, genomic instability, etc. Over the last half-century, the United States Food and Drug Administration (USFDA) has approved more than one hundred drugs for clinical treatment of cancers. Nevertheless the search for new and/or improved chemical compounds as potential anticancer agents continues with the hope that better efficacy and more manageable adverse side effects of pharmaceutical drugs may be achieved. Molecular modeling, screening and mimicking of natural compound derivatives have been among several drug discovery approaches to rationally design and modified structures that may confer a better therapeutic index[8] or that can cure cancer in the human race[9].

Among such compounds are pyrazole and its derivatives, pyrazoles are class of heterocyclic compounds used for the development of drugs, and they have attracted the attention of several researchers due to their extensive biotic actions such as anticancer[10], antifungal[11], antiviral[12], anti-inflammatory[14,15]. More so, pyrazole derivatives such as Pyrazolopyrimidine and pyrazolo[4,3-*d*]pyrimdin-7-one perform some pharmacological activities which can never be put aside in the medical world, for example as antihypertensive[15], antiviral[16,17], tuberculostatic[18], herbicidal agents[19], antileishmanial[20] and treatment of heart diseases[21]. Therefore, the structural features of the Pyrazoles have been recognized as vital parameters due to their bioactivity as therapeutic aids. Several pyrazoles have been commercialized such as omeprazole, Albendazole, mebendazole, candesartan, telmisartan, astemizole[22-24].

Quantitative Structural Activity Relationship (QSAR) as a statistical model embroils the relationship between physicochemical parameters of a chemical compound to its biological activity[25]. It has attracted vast usefulness for linking molecular evidence with biotic activities and many other physicochemical properties as well as its helpfulness for drug design, discovery, and development[26]. QSAR helps in the prediction of toxicity of materials in bulk system, for instance, drug-like compounds and are very useful in case of the classic chemicals[27-30]. The use of molecular descriptors calculated from quantum chemical methods for development of QSAR models has been described to be sufficient for generating comprehensive QSAR. Thus

Author α: Department of Pure and Applied Chemistry, Ladoke Akintola University of Technology, Ogbomoso, Nigeria.
e-mail: bsemire@lautech.edu.ng

the use of quantum chemical descriptors has countless potential[31-34].

Molecular docking studies divulge information on the interaction between the drug-like compound known as a ligand and an enzyme/receptor through recognizing the active positions within the enzyme along with the binding energy calculation[34]. In molecular docking, scoring is a statistical way of predicting the strength of the interactions which are non-covalent in between a ligand and a receptor. Therefore, the calculations of interaction energy can be offered in the form of "dock score"[35].

Consequently, in this research, twenty pyrazole derivatives with known anti-colon cancer activities[21] as displayed in Figure 1 were optimized using Density Functional Theory (DFT) method so as to obtain molecular descriptors for the compounds. These compounds are 4-amino-3-(4-chlorophenyl)-1H-pyrazolyl-5-yl- (3,5-dimethyl-1Hpyrazol-1 yl) derivatives) methanone (**3a, b**), 2-{[4-amino-3-(4-chlorophenyl)-1H-pyrazol-5-yl]carbonyl}-5-methyl-2,4-dihydro-3H-pyrazol-3-one (**4**), 1-{[4-amino-3-(4-chlorophenyl-1H-pyrazol-5-yl]carbonyl} pyrazolidine- 3,5- dione (**5**), 3-(4-chlorophenyl)-5-(1,3,4-oxa/thiadiazol-2yl)-1H-pyrazol-4-amine (**7a, b**), 6-amino-3-(4-chlorophenyl)-5-methyl-1,6-dihydro-7*H*-pyrazolo-[4,3-*d*]pyrimidin-7-one (**9**), 4-amino-3- (4-chlorophenyl)- N'- [arylmethylidene]- 1H-pyrazole-5-carbhydrazide ***(10 a-d)***, 3-(4-chlorophenyl)-5-methyl-1,6-dihydro-7*H*-pyrazolo[4,3-*d*]pyrimidine-7-one (**12**), 7- chloropyrazolo [4,3-*d*] pyrimidine (**13**), 3-(4-chlorophenyl)-7-(3,6-dihydro-2H-pyran-4-yl)-5-methyl-1H-pyrazolo[4,3-d]pyrimidine (**14**),7- (4-chlorophenyl)-5-methyl -9H-pyrazolo[3,4-e]tetrazolo[1,5-c]pyrimidine ***(15)***, Ethyl{[3- (4-chlorophenyl)- 5- methyl- 1H- pyrazolo [4,3-d]pyrimidine-7-yl]oxy} acetate (***16)***, 6-amino-3-(4-chlorophenyl)- 5- thioxo- 1,4,5,6- tetrahydro- 7*H*-pyrazolo[4,3-*d*] pyrimidin-7-one (**17**), 2-{[4-amino-3-(4-chlorophenyl)- 1H- pyrazol- 5- yl] carbonyl} hydrazinecarbothioamide (***18),*** 4-amino-3-(4-chlorophenyl)-N'-(4-methyl/ or 4-phenyl-1,3-thiazol-2-yl)-1*H*-pyrazole-5-carbohydrazide (**19a, b**). Thus, the major objectives of this work are: (i) to calculate molecular descriptors with the use of quantum chemical method via Density Functional Theory (DFT), (ii) to develop QSAR model which probe into biological activity of the studied compounds, and (iii) to calculate the free energy of interactions (binding affinity, ΔG) of the ligand with the receptor in the binding site through molecular docking.

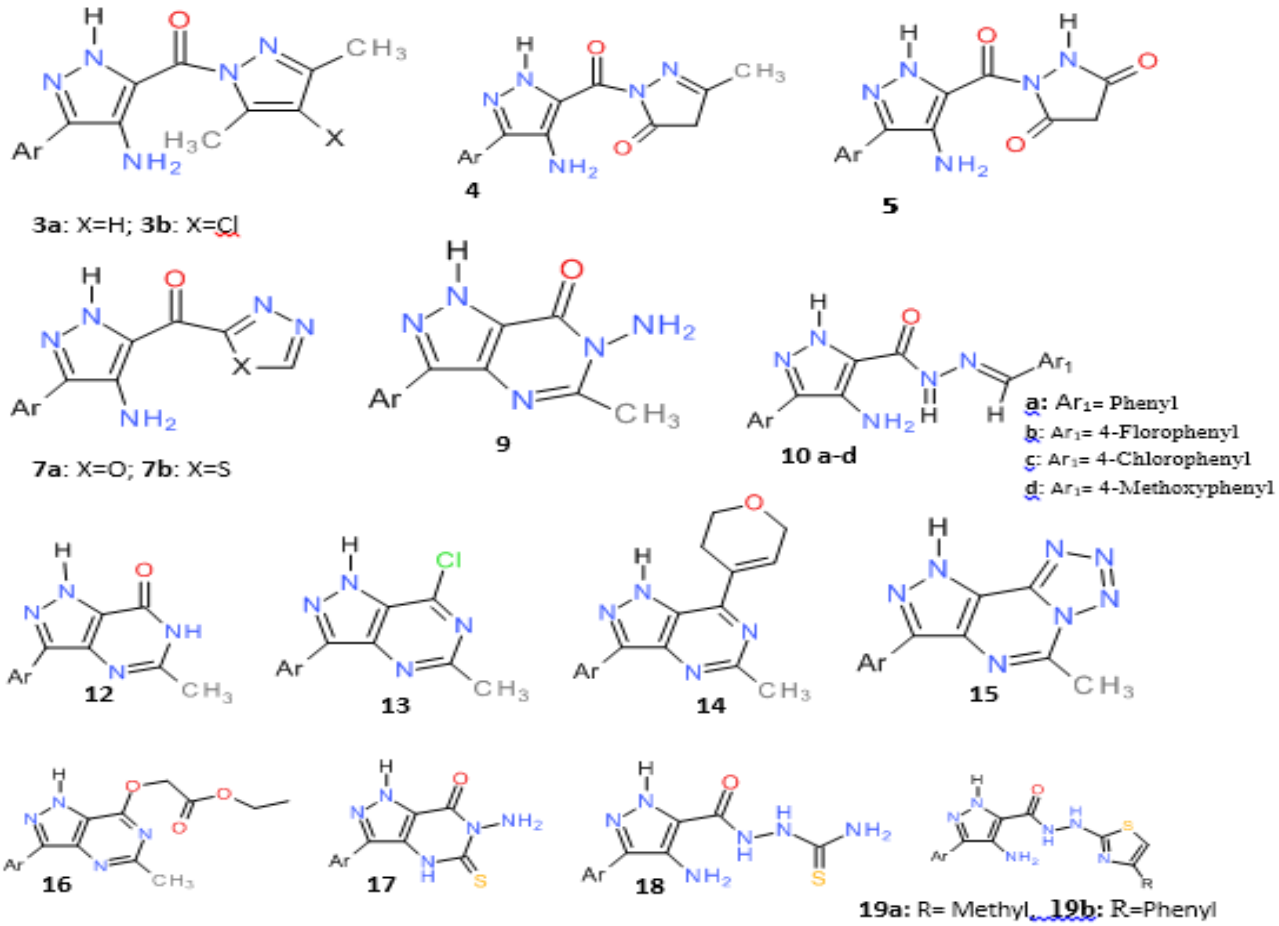

Figure 1: The schematic structures of the pyrazole derivatives, the compounds were numbered as used in [20]

II. Computational Details

a) Ligand optimization and molecular descriptors

The equilibrium geometries for the twenty pyrazole derivatives as reflected in this paper were optimized at Density Functional Theory (DFT). The use of DFT method entails three-parameter density functional, which comprises Becke's gradient exchange correction[37] and the Lee, Yang, Parr correlation functional (i.e., B3LYP)[38]. The accuracy of DFT calculations depends on the particular functional chosen and basis sets. However, 6-31G** basis set has been found to be appropriate for the confirmation search and calculation of drug-like compounds[39]. Therefore 6-31G** basis set was used in this work. Also, the optimized compounds were used to calculate molecular parameters/descriptors that described the bioactivity (IC_{50}) of the compounds. The optimized molecular structures were used for the docking study to estimate the binding affinity of the compounds to the colon cancer cell line, HT29 receptor (PDB ID: 2N8A). The optimization of the compounds was carried out using quantum chemical software Spartan '14 by wavefunctionInc[40].

Table 1: Calculated descriptors used in this study

Descriptors	Symbol	Abbreviation
Quantum chemical descriptors	Molecular dipole moment	DM
	Molecular polarizability	P
	Highest occupied molecular orbital, eV	HOMO
	Lowest unoccupied molecular orbital, eV	LUMO
	Solvation energy (au)	SE
	Natural charge population on nitrogen atoms of pyrazole ring in *e* (Het)	(N+N)/2
	Difference between E_{LUMO} and E_{HOMO}, eV	BD
	Chemical Hardness [$\eta = 1/2 (E_{HOMO} + E_{LUMO})$] eV	η
	Softness ($S = 1/\eta$) eV^{-1}	S
	Electro negativity [$\mu = 1/2 (E_{HOMO} - E_{LUMO})$] eV	μ
	Nucleophilicity ($\omega = \mu^2/2\eta$) eV	ω
Chemical properties	Partition Coefficient	Log P
	Molecular weight	MW
	Volume	V
	Ovality	Ovl
	Polar surface area	PSA
	Bond length between two Nitrogen atoms of the pyrazole ring	NNBL
	Bond length between Nitrogen and the hydrogen atom of pyrazole ring	NHBL
	Natural charge population on Hydrogen atoms of the pyrazole ring	H HET4r
	Hydrogen bond donor	HBD
	Hydrogen bond acceptor	HBA

b) Data processing and QSAR modeling

Furthermore, the chosen calculated parameters were engaged to develop quantitative structure-activity relationship (QSAR) model to link the bioactivity to the calculated molecular descriptors obtained from the studied compounds[41]. This was achieved using multiple linear regression (MLR) method which is a recurrent statistical technique used in developing QSAR model. MLR and correlation analyses were carried out by the statistics software SPSS 13.0 version. Before MLR analysis, the person correlation table was used to examine collinearity among the descriptors ($r > 0.90$). The descriptors with higher correlation with the dependent variable (IC_{50}] were retained, and the others were removed from the descriptor data matrix. The remaining descriptors were used to construct the MLR model, by the stepwise method. Moreover, the QSAR model was validated using some statistical equations such as cross validation (R^2) and adjusted R^2. Cross validation is a mathematical method which oversees the reliability of QSAR model that can be used for a set of facts as shown in equation 1.

$$\mathrm{CV.R^2} = 1 - \frac{\sum(\mathrm{Y_{obs}} - \mathrm{Y_{cal}})^2}{\sum(\mathrm{Y_{obs}} - \bar{\mathrm{Y}}_{\mathrm{obs}})^2} \quad (1)$$

The adjusted R^2 could be calculated using equation (2)

$$\mathrm{R_a^2} = \frac{(\mathrm{N-I})\times\mathrm{R^2-P}}{\mathrm{N-P-1}} \quad (2)$$

where N is number of observations (compounds), *p* is number of descriptors,

Also, for a good model, the standard error of estimate (s) of a set of data should be low, and this is defined as follows:

$$s = \sqrt{\frac{\sum(Y_{obs} - Y_{cal})^2}{N-p-1}} \quad (3)$$

To judge the overall significance of the regression coefficients, the variance ratio (F) which is the ration of regression mean square to deviations mean square can be defined as follows:

$$F = \frac{\frac{\sum(Y_{cal} - \bar{y}_{obs})^2}{p}}{\frac{\sum(Y_{obs} - Y_{cal})^2}{N-p-1}} \quad (4)$$

The F value has two degrees of freedom: p, N − p − 1. The computed F value of a model should be significant at $p < 0.05$; thus for overall significance of the regression coefficients, the F value should be high.

c) Molecular Docking and binding affinity

The downloaded **HT29** receptor (**PDB ID: 2N8A**[42]) from protein data bank was treated i.e., removal of water molecules, ligand, and cofactors from the receptor with the use of discovery studio. Then, both the receptor and ligand were converted to the acceptable format (pdbqt) for AutoDockvina programme. The grid dimension used for all the 2N8A protein was are 50 × 40 ×40 Å (grid size) with point separated by 1.000 Å (grid-point spacing). The docking was done using autodock vina which was inspired by Darwinian evolution theory to be iterative optimization method[43] which involves search Algorithm. At the completion of the docking runs, ligand showing different conformations known as Binding modes were obtained with their respective binding affinity. The stable pattern was assumed to be the one with the lowest binding affinity and was taken for post-docking analysis using Edupymol version 1.7.4.4.

III. Result and Discussion

a) QSAR modeling

The molecular descriptors calculated for the twenty pyrazole compounds served as independent variables, while the observed inhibitory actions ($IC_{50,}\mu M$) against cancer cells line as the dependent variable in the development of QSAR model via multiple linear regression (MLR). These molecular descriptors used for QSAR model were displayed in Tables 2 and 3. In QSAR study, the quality of a model is evaluated by its fitting and prediction abilities; however, for a model to be acceptable, its predictability power is of paramount important. Therefore, Pearson's matrix was used for the selection of suitable descriptors for the QSAR study (Table 4).

Table 2: The calculated molecular descriptors from the compounds

MOL	HOMO	LUMO	BG	DM	SE (au)	(N+N)/2 Het	η	μ	ω
3a	-5.54	-1.66	3.98	5.26	-0.01389	-0.379	3.600	-1.940	0.5227
3b	-5.66	-1.85	3.81	3.33	-0.01208	-0.379	3.755	-1.905	0.4832
4	-5.87	-1.60	4.27	6.35	-0.02134	-0.353	3.735	-2.135	0.6102
5	-6.58	-1.94	4.64	2.54	-0.03482	-0.355	4.260	-2.455	0.7074
7a	-5.74	-1.41	4.33	3.51	-0.02187	-0.398	3.575	-2.165	0.6556
7b	-5.66	-1.80	3.86	3.76	-0.01747	-0.399	3.730	-1.930	0.4993
9	-5.96	-1.36	4.60	4.23	-0.01815	-0.405	3.660	-2.300	0.7227
10a	-5.84	-0.82	5.02	5.19	-0.01575	-0.368	3.330	-2.510	0.9460
10b	-5.84	-1.65	4.33	1.68	-0.01442	-0.368	3.815	-2.165	0.6143
10c	-6.07	-1.80	4.27	1.81	-0.01671	-0.377	3.935	-2.135	0.5792
10d	-5.56	-1.44	4.12	2.91	-0.01841	-0.368	3.500	-3.128	1.3973
12	-5.99	-1.31	4.68	4.11	-0.01977	-0.401	3.650	-2.340	0.7501
13	-6.23	-2.09	4.14	2.26	-0.01402	-0.413	4.160	-2.070	0.5150
14	-5.91	-2.09	3.82	4.67	-0.01784	-0.427	4.000	-1.910	0.4560
15	-5.91	-1.99	4.39	0.76	-0.01789	-0.424	4.185	-2.195	0.5756
16	-5.88	-1.45	4.43	6.68	-0.01861	-0.418	3.665	-2.215	0.6693
17	-6.18	-1.89	4.29	3.02	-0.02548	-0.391	4.035	-2.145	0.5701
18	-5.79	-1.41	4.38	4.84	-0.03355	-0.396	3.600	-2.190	0.6661
19a	-5.73	-1.24	4.49	4.68	-0.02043	-0.372	3.485	-2.245	0.7231
19b	-5.70	-1.30	4.40	4.39	-0.02085	-0.371	3.485	-2.200	0.6914

Table 3: The calculated molecular descriptors from the compounds (Continued)

MOL	MW	Vol	Ova	Log P	PSA	Pol	NNBL	NHBL	H HET4r	HBD	HBA
3a	315.764	297.32	1.48	0.07	63.211	64.57	1.322	1.012	0.294	2	6
3b	350.209	310.90	1.51	-0.06	63.228	65.69	1.322	1.011	0.294	2	6
4	317.736	287.79	1.48	-1.01	85.752	63.71	1.320	1.010	0.296	3	7
5	319.708	275.32	1.46	-1.52	100.075	62.61	1.329	1.010	0.300	3	8
7a	261.672	229.28	1.39	0.26	74.597	58.95	1.333	1.008	0.285	2	6
7b	277.739	238.68	1.40	0.83	64.537	59.82	1.334	1.008	0.282	2	6
9	275.699	246.62	1.42	-0.15	72.744	60.29	1.345	1.008	0.292	2	5
10a	341.802	329.28	1.55	0.60	88.836	66.90	1.329	1.010	0.292	3	6
10b	357.776	327.84	1.45	1.62	79.201	66.94	1.334	1.010	0.294	3	6
10c	374.231	337.13	1.55	2.02	79.118	67.71	1.336	1.010	0.295	3	6
10d	369.812	350.35	1.57	1.34	86.232	68.82	1.333	1.010	0.293	3	7
12	260.684	235.01	1.39	0.10	56.316	59.33	1.345	1.008	0.294	1	4
13	279.130	241.38	1.40	1.55	37.704	59.98	1.354	1.008	0.292	1	4
14	326.787	311.07	1.47	1.67	42.724	65.70	1.352	1.006	0.277	1	5
15	285.698	246.93	1.40	1.83	68.584	60.37	1.352	1.008	0.297	1	6
16	332.747	303.52	1.52	0.76	64.473	64.95	1.351	1.007	0.287	1	6
17	293.738	244.92	1.41	0.15	74.925	60.23	1.339	1.009	0.300	3	7
18	310.679	266.54	1.49	-0.96	106.292	61.96	1.335	1.009	0.287	5	8
19a	348.818	309.47	1.53	0.09	89.093	65.42	1.327	1.009	0.292	3	7
19b	410.889	374.88	1.59	1.49	88.388	70.75	1.327	1.009	0.293	3	7

Table 4: Pearson's correlation matrix

	HT29	HOMC	LUMC	BG	DM	SE	N+N/2HE	CP	CH	GN	MW	VOI	OVA	LOGP	PSA	POL	NNBL	NHBL	HHET4r	HBD	HBA
HT29	1.000																				
HOMO	-0.009	1.000																			
LUMO	0.306	0.476	1.000																		
BG	0.334	-0.349	0.655	1.000																	
DM	0.280	0.520	0.506	0.102	1.000																
SE	-0.370	0.372	-0.028	-0.342	-0.064	1.000															
N+N/2HET	0.274	0.152	0.320	0.219	0.060	-0.173	1.000														
CP	-0.434	0.005	-0.448	-0.472	0.092	0.229	-0.343	1.000													
CH	-0.191	-0.828	-0.888	-0.235	-0.596	-0.177	-0.284	0.283	1.000												
GN	0.423	0.230	0.567	0.397	0.039	-0.111	0.356	-0.970	-0.48	1.000											
MW	0.283	0.285	0.195	-0.044	0.044	0.125	0.533	-0.225	-0.27	0.284	1.000										
VOL	0.295	0.365	0.272	-0.027	0.130	0.233	0.499	-0.272	-0.36	0.355	0.973	1.00									
OVALITY	0.456	0.419	0.414	0.078	0.303	0.061	0.501	-0.349	-0.48	0.442	0.913	0.92	1.00								
LOGP	-0.292	0.049	-0.199	-0.266	-0.375	0.587	-0.434	0.018	0.107	0.018	0.257	0.29	0.15	1.000							
PSA	0.524	0.033	0.483	0.482	0.081	-0.631	0.672	-0.459	-0.32	0.439	0.392	0.31	0.45	-0.488	1.000						
POL	0.288	0.372	0.258	-0.047	0.128	0.240	0.494	-0.262	-0.36	0.347	0.973	1.00	0.91	0.304	0.300	1.000					
NNBL	-0.095	-0.463	-0.331	0.031	-0.245	0.078	-0.861	0.044	0.454	-0.13	-0.422	-0.39	-0.44	0.488	-0.580	-0.395	1.000				
NHBL	0.240	0.221	0.135	-0.013	-0.074	0.098	0.787	-0.137	-0.20	0.174	0.402	0.38	0.38	-0.334	0.435	0.381	-0.802	1.000			
HHET4r	0.088	-0.447	-0.027	0.374	-0.354	-0.135	0.527	-0.289	0.251	0.164	0.143	0.05	0.05	-0.260	0.347	0.050	-0.293	0.606	1.000		
HBD	0.565	0.168	0.346	0.219	0.066	-0.541	0.655	-0.273	-0.30	0.294	0.417	0.32	0.44	-0.432	0.873	0.323	-0.600	0.501	0.234	1.000	
HBA	0.416	0.048	0.131	0.097	0.096	-0.658	0.579	-0.263	-0.10	0.247	0.422	0.30	0.44	-0.451	0.861	0.305	-0.583	0.410	0.267	0.787	1.000

The selected descriptors were used to build a linear QSAR model to understand how multiple linear regression (MLR) equations can explain the structural key points correlating to differential behavior in bioactivity against colon cancer cell (HT29) as shown in equation 4. This model was validated statistically by using the squared fitting factor (R^2), cross validation ($CV.R^2$), adjusted fitting factor ($_{adj}R^2$) and variation ratio (F). The developed model was very robust in predicting satisfactory the experimental values. The high values of F, R^2, $CV.R^2$ and $_{adj}R^2$ as shown in Table 5 indicated that the models are statistically acceptable and also have good external predictability[44,45]. The calculated R^2 is 0.9564; this revealed a reasonable fitness, and it also uncovered the efficiency of the model as displayed in equation 4. The value for $CV.R^2$ was calculated to be 0.9542 which is greater than 0.5 (standard)[46], and this showed the reliability and acceptability of the model as well as the adjusted R^2 with 0.9247 which was greater than 0.6 (Table 5)

$$IC_{50} = -2677.65 - 38.6214(BG) + 0.864947(DM) + 257.863(NNBL) + 2353.57(NHBL) - 190.240(HHET4r) - 39.6798(HOMO) + 37.8067(LUMO) + 0.0699416(PSA) \quad (4)$$

The QSAR model contained eight descriptors in different combinations; each descriptor with either positive or negative coefficient attached to it. However, the magnitudes of the coefficients as well as, the values of descriptors have significant roles in deciding the overall biological activity of the molecule. The descriptors with negative coefficients in the model were very significant because they contributed towards increasing the value of the biological activity of anti-colon cancer agents. Therefore, the descriptors with a negative coefficients were most significant followed by descriptors with low weight positive coefficients and lastly the parameters with high weight positive coefficients. The predicted anti-colon cancer activity of the ligands using the QSAR model as well as deviation from the experimental values was displayed in Table 6 and graphically presented in Figures 2 and 3.

Table 5: Statistical parameters for validation of QSAR model

N	p	R^2	$CV.R^2$	R^2_{adj}	s	F
20	8	0.9564	0.9542	0.9247	0.4141	30.168

Table 6: Stepwise regression result for anti-colon cancer activity

Comp	Observed	Predicted	Residual	Comp	Observed	Predicted	Residual
3A	1.45	1.45	-0.00	10D	3.57	3.05	0.52
3B	1.10	1.57	-0.47	12	0.78	0.54	0.24
4	2.78	2.53	0.25	13	1.52	1.23	0.29
5	2.99	2.82	0.17	14	0.88	0.96	-0.08
7A	0.28	-0.26	0.54	15	0.29	0.70	-0.41
7B	0.20	0.31	-0.11	16	3.88	3.86	0.02
9	1.77	2.19	-0.42	17	1.33	1.24	0.09
10A	4.08	4.16	-0.08	18	5.59	5.65	-0.06
10B	2.10	2.18	-0.08	19A	0.42	1.09	-0.67
10C	2.92	2.83	0.09	19B	0.78	0.62	0.16

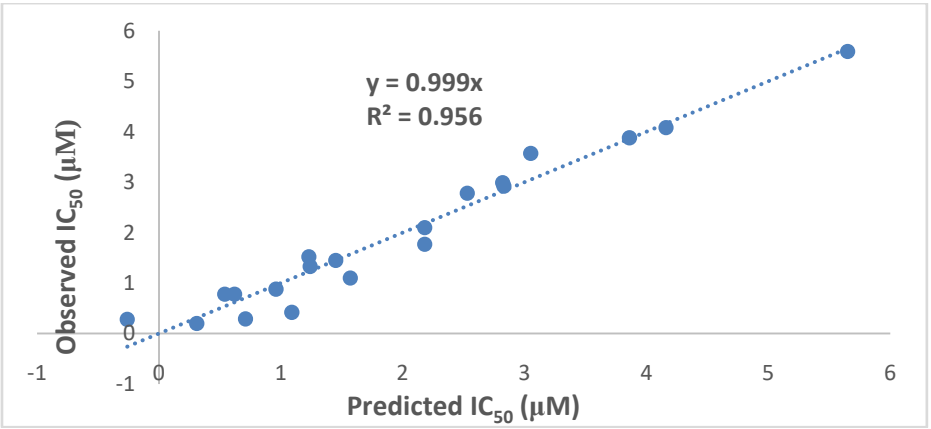

Figure 2: The calculated predicted IC_{50} against the experimental IC_{50}.

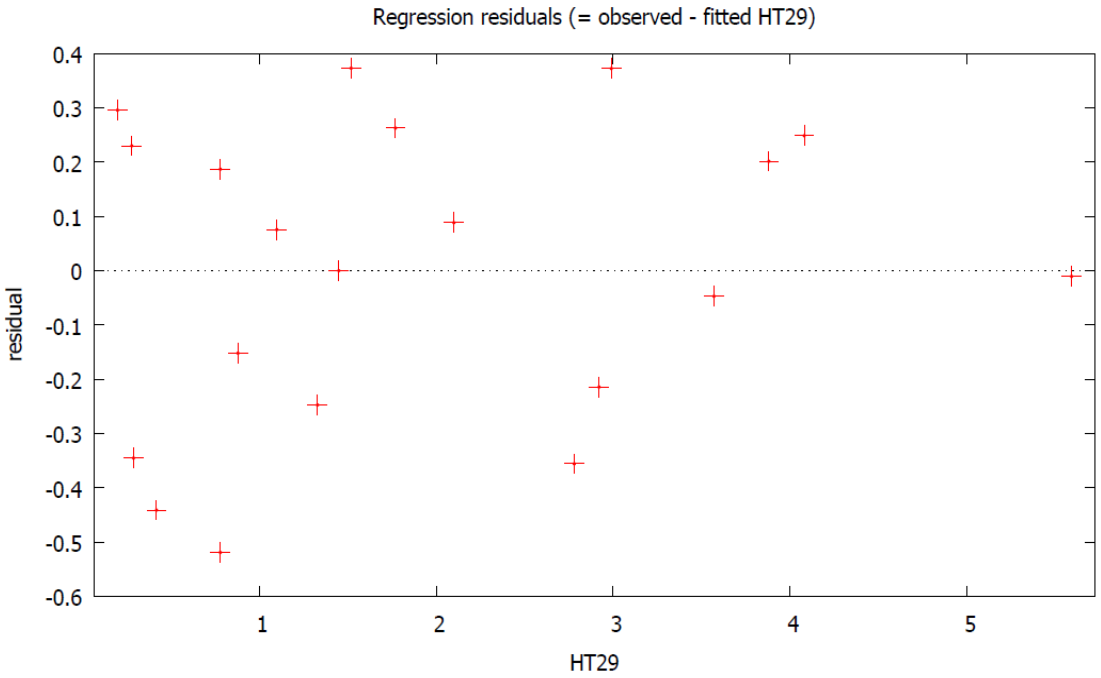

Figure 3: The residuals versus observed IC_{50}

b) Docking and Scoring

The molecular docking studies were performed on the twenty pyrazole derivatives together with colon cancer cells line (PDB ID: 2N8A)[42] obtained from protein data bank. This was achieved with the use of several software such as Discovery studio, Autodock tool, Autodock vina and Pymol as post-dock software. Docking of each compound was carried using autodock vina and conformations obtained varies in number but ranged from 8 – 15 conformations for compounds 3a-19b. The structure with lowest binding energy (i.e., highest negative free energy of binding, ΔG) in each docking simulation was taken to be most stable and analyzed for detailed interactions using Discovery Studio Visualizer4.0 software. Docking simulations can be understood by comparing the values of the free energy of binding (Gibbs energy, ΔG) of the ligands to the protein receptor. ΔG is an indicator to show the stability interaction between ligand and receptor, and it can be used to explain the strength of binding energies of different docking conformation[47,48].

The poses of the lowest conformation of each ligand were examined based on ΔG, and interaction of the ligand with the **2N8A** protein structure in ligand-receptor complex. The free binding energy (ΔG) calculated for the docked twenty pyrazole derivatives ranged from -6.10 kcal/mol (ligand **7a**) to -8.20 kcal/mol (ligand **19b**) as displayed in Table 7. The interaction of ligand with the **2N8A** protein structure was discussed by of H-bonding between the ligand and the receptor molecule as shown in Figure 4. Analysis of the ligand-receptor complex showed that H-bonds played a prominent role in the binding and posed stability of the ligand in the ligand-receptor complex; thus affect the potency/function of biological molecules. The number of H-bonds present in the ligand-protein complex as well as H-bonds distances was shown in Table 7. The ligand **3a** formed one H-bond with **2N8A** receptor involving GLN-40 and LIG: O (carbonyl oxygen) with the bond distance of 2.3 Å; whereas two H-bonds were observed for **3b** with GLN-40 H-bonded to carbonyl oxygen with 2.5 Å bond length and also with hydrogen atoms on N-H of pyrazole ring with 1.8 Å.

Furthermore, ligand **4** two H-bonds, with ALA-64 H-bonded to hydrogen N-H of pyrazole ring of the ligand with 2.5 Å distance apart, and THR-109/LIG:O (pyrazole-carbonyl oxygen) with 1.9 Å bond length. For ligand 5, five H-bonds were observed with ALA-89/LIG:O (pyrazole-carbonyl oxygen) with the distance of 3.0 Å, ILE-64/LIG: O (one of the carbonyl oxygen of pyrazolidine-3,5-dione) with the distance of 3.6 Å, and GLU-107/LIG:O (pyrazole-carbonyl oxygen) with distance of 3.1 Å. Others were GLU-107/LIG:H (hydrogen of N-H of pyrazole ring) with distance of 2.5 Å, GLU-107/LIG:N (amino group of pyrazole ring) with 3.2 Å bond distance, LYS-108/LIG:N (amino group of pyrazole ring) with distance 2.2 Å, and THR-109/LIG:N (amino group of pyrazole ring) with distance 2.8 Å as well as THR-109/LIG:H (H-amino group of pyrazole ring) with distance 2.2 Å.

Table 7: Interactions between ligands and **2N8A** receptor

Comp	Affinity (kcal/mol)	H-Bond Between protein residues in the binding pocket and Drug	Distance
3a	-7.1	GLN-40, LIG:O	2.3
3b	-7.4	(i) GLN-40, LIG:O (ii) GLN-40, LIG:H	(i)2.5 (ii) 1.8
4	-7.1	(i) ALA-106, LIG: H (ii) THR-109, LIG:O	(i) 2.5 (ii) 1.9
5	-6.9	(i) ALA-89, LIG:O (ii) ILE-64, LIG: O (iii) GLU-107, LIG: O (iv) GLU-107, LIG: H (v) GLU-107, LIG:N (vi) LYS-108, LIG:N (vii) THR-109, LIG:N (viii) THR-109, LIG: H	(i) 3.0 (ii) 3.6 (iii) 3.1 (iv) 2.5 (v) 3.2 (vi) 2.2 (vii) 2.8 (viii) 2.2
7a	-6.1	LYS-47, LIG: N	(i) 2.4
7b	-6.4	(i) MET-38, LIG: H (ii) GLN-40, LIG:H	(i) 2.4 (i) 2.3
9	-6.8	(i) THH-109, LIG:N (ii) GLU-107, LIG:H(iii) GLU-107, LIG:H (iv) GLU-107, LIG: O (v) ALA-89, LIG: O (vi) ILE-64 LIG: O (vii) ILE-64, LIG: H	(i) 3.0 (ii) 2.9 (iii) 2.1 (iv) 3.4 (v) 3.2 (vi) 3.6 (vii) 2.5
10a	-7.4	(i) THR-109, LIG: O (ii) GLU-90, LIG:H (iii) GLU-90, LIG: H (iv) ALA-89, LIG: H	(i) 3.3 (ii) 2.1 (iii) 2.7 (iv) 2.0
10b	-7.2	(i) THR-88, LIG: H, (ii) ALA-91, LIG: H	(i) 2.8 (ii) 2.5
10c	-7.2	(i) THR-176, LIG: H (ii) THR-109, LIG: H (iii) GLU-107, LIG:H (iv) GLU-107, LIG: O (v) ARG-65, LIG:O	(i) 2.1 (ii) 2.6 (iii) 2.5 (iv) 2.1 (v) 2.2
10d	-7.5	(i) ARG-65, LIG:O (ii) GLY-111, LIG:O (iii) THR-109, LIG:H (iv) GLU-107, LIG:H (v) GLU-107, LIG: N	(i) 2.3 (ii) 2.2 (iii) 2.1 (iv) 2.4 (v) 2.8
12	-6.4	(i) THR-109, LIG: O (ii) THR-109, LIG:H	(i) 3.3 (ii) 2.2
13	-6.4	MET-38, LIG:H	(i) 2.2
14	-7.0	(i) ASP-6, LIG: H (ii) THR-109, LIG:H	(i) 2.4 (ii) 2.5
15	-7.3	(i) GLU-107, LIG:H (ii) THR-109, LIG: N (iii) THR-109, LIG: N (iv) LYS-108, LIG: N (v) LYS-108, LIG: N	(i) 2.5 (ii) 2.0 (iii) 2.7 (iv) 1.9 (v) 2.1
16	-6.4	LYS-47, LIG: O	2.4
17	-6.8	(i) ALA-89, LIG:H (ii) ALA-89, LIG: O (iii) ILE-64, LIG:O (iv) GLU-107, LIG: O (v) GLU-107, LIG: H (vi) THR-109, LIG: N	(i) 2.2 (ii) 3.2 (iii) 3.5 (iv) 3.4 (v) 2.1 (vi) 3.0
18	-6.8	(i) GLY-93, LIG:N (ii) GLU-90,LIG:H (iii) GLU-90, LIG:H (iv) GLU-107, LIG:H (v) GLU-107, LIG:H (vi) GLU-107, LIG:H (vii) GLU-107, LIG: H (viii) GLU-90, LIG:H (ix) ALA-89, LIG:H (x) GLU-107, LIG:H (xi) GLU-107, LIG: H	(i) 3.5 (ii) 2.5 (iii) 2.2 (iv) 2.1 (v) 2.2 (vi) 2.6 (vii) 2.4 (viii) 2.5 (ix) 2.5 (x) 2.5 (xi) 2.8
19a	-7.2	(i) ALA-106, LIG: N (ii) ALA-106, LIG:H (iii) GLU-107, LIG: H (iv) GLU-107, LIG: H (v) GLU-90, LIG: H (vi) GLY-93, LIG: H	(i) 3.4 (ii) 2.7 (iii) 2.2 (iv) 2.0 (v) 2.2 (vi) 2.3
19b	-8.2	(i) THR-109, LIG: O (ii) THR-109, LIG:O (iii) LYS-108, LIG: O (iv) GLU-107, LIG:H (v) GLU-107, LIG:H (vi) GLU-107 LIG: H (vii) ALA-106, LIG: H (viii) GLU-90, LIG: H	(i) 2.3 (ii) 2.8 (iii) 2.0 (iv) 2.9 (v) 2.4 (vi) 2.5 (vii) 2.5 (viii) 2.0

However, for ligand **7a**, one H-bond was observed between LYR-47 and LIG:N (amino group of pyrazole ring); whereas two H-bonds for **7b** with MET-38/LIG:H (hydrogen of N-H of pyrazole ring) with distance of 2.9 Å, and GLN-40/LIG:H (H-amino group of pyrazole ring) with distance 2.3 Å. Seven H-bonds were observed for ligand **9;** THR-109/LIG:N (amino-group of pyrazole ring), GLU-107/LIG:H (H-amino group of pyrazole ring), GLU-107/LIG:H (hydrogen of N-H of pyrazole ring), GLU-107/LIG: O (Carbonyl oxygen of pyrimidinone). Others were ALA-89/LIG: O (Carbonyl oxygen of pyrimidinone), ILE-64/LIG:O (Carbonyl oxygen of pyrimidinone) and ILE-64/LIG: H (hydrogen N-H of pyrazole ring) with distance of 2.5 Å. Also, four H-bonds were observed for ligand **10a;** THR-109/LIG: O(pyrazole-carbonyl oxygen), GLU-90/LIG:H (hydrogen of N-H of carboxamide), GLU-90/LIG:H (H-amino group of pyrazole ring) and ALA-89/LIG:H (hydrogen of N-H of pyrazole ring). Two H-bonds were observed in docked complex of ligand **10b** and receptor**;** THR-88/LI G: H (H-amino group of pyrazole ring) and ALA-91/LIG:H (hydrogen of N-H of pyrazole ring). For ligand **10c**, five H-bonds were observed via THR-176/LIG:H (hydrogen of N-H of carboxamide), THR-109/LIG:H (H-amino group of pyrazole ring), GLU-107/LIG:H (hydrogen of N-H of pyrazole ring), GLU-107/LIG:O (pyrazole-carbonyl oxygen) and ARG-65/LIG:O (pyrazole-carbonyl oxygen). Also, five H-bonds were recorded for ligand **10d**; ARG-65/LIG:O (pyrazole-carbonyl oxygen), GLY-111/LIG:O (pyrazole-carbonyl oxygen), THR-109/LIG:H (H-amino group of pyrazole ring), GLU-107/LIG:H (hydrogen of N-H of pyrazole ring) and GLU-107/LIG: N (amino group of pyrazole ring).

Likewise, ligand **12**receptor complex presented two H-bonds; THR-109/LIG:O (Carbonyl oxygen of pyrimidin-one) and THR-109/LIG:H (hydrogen of N-H of pyrazole ring); whereas MET-38 was H-bonded with hydrogen of N-H of pyrazole ring of the ligand **13** with bond distance of 2.2 Å. For ligand **14,** two H-bonds were observed in the ligand-receptor complex; ASP-6/LIG:H (hydrogen of N-H of pyrazole ring) with the distance of 2.4 Å and THR-109/LIG:H (hydrogen of N-H of pyrazole ring) with of distance 2.5 Å. Also, for ligand **15**, five H-bonds were identified through GLU-107/LIG:H (hydrogen of N-H of pyrazole ring), THR-109/LIG: N (triazolyl ring), THR-109/LIG: N (N of N-H of pyrazole ring), LYS-108/LIG: N (one of N of triazolyl ring) and LYS-108/LIG: N (one of N of triazolyl ring). Moreover, one H-bond was observed for ligand **16**–receptor complex viaLYS-47/LIG:O(carboxylic-group) with H-bond distance of 2.4 Å; whereas for ligand **17**-receptor complex, six H-bonds were detected. The H-bonds were ALA-89/ LIG:H (hydrogen of N-H of pyrazole ring), ALA-89/LIG:O (First ketonic-group of pyrimidine-dione ring), ILE-64/LIG:O (Second Ketonic-group of pyrimidine-dione ring), GLU-107/LIG:O (First ketonic-group of pyrimidine-dione ring), GLU-107/LIG:H (hydrogen of N-H of pyrazole ring) and THR-109/LIG:N (N of N-H of pyrazole ring).

Also, for ligand **18**, eleven H-bonds were detected between the ligand and receptor residues vis-à-vis GLY-93/LIG:N, GLU-90/LIG:H, GLU-90/IG:H, GLU-107/LIG:H, GLU-107/LIG:H, GLU-107/LIG:H, GLU-107/ LIG: H, GLU-90/LIG:H, ALA-89/LIG:H, GLU-107/LIG:H and GLU-107LIG:H. Similarly, for ligand **19a** formed six H-bonds with **2N8A;** ALA-106/LIG: N, ALA-106/LIG:H, GLU-107/LIG: H, GLU-107/LIG:H, GLU-90/LIG:H, GLY-93/LIG:H. However, for ligand **19b,** eight H-bonds were observed between the ligand and **2N8A** residues. These were THR-109/LIG:O, THR-109/LIG:O, LYS-108/LIG:O, GLU-107/LIG:H, GLU-107/LIG:H, GLU-107/LIG:H, ALA-106/LIG:H and GLU-90/LIG: H. Some selected ligand – receptor (2N8A) complexes showing stable conformation, as well as Van Waal interactions, were displayed in Figure 4.

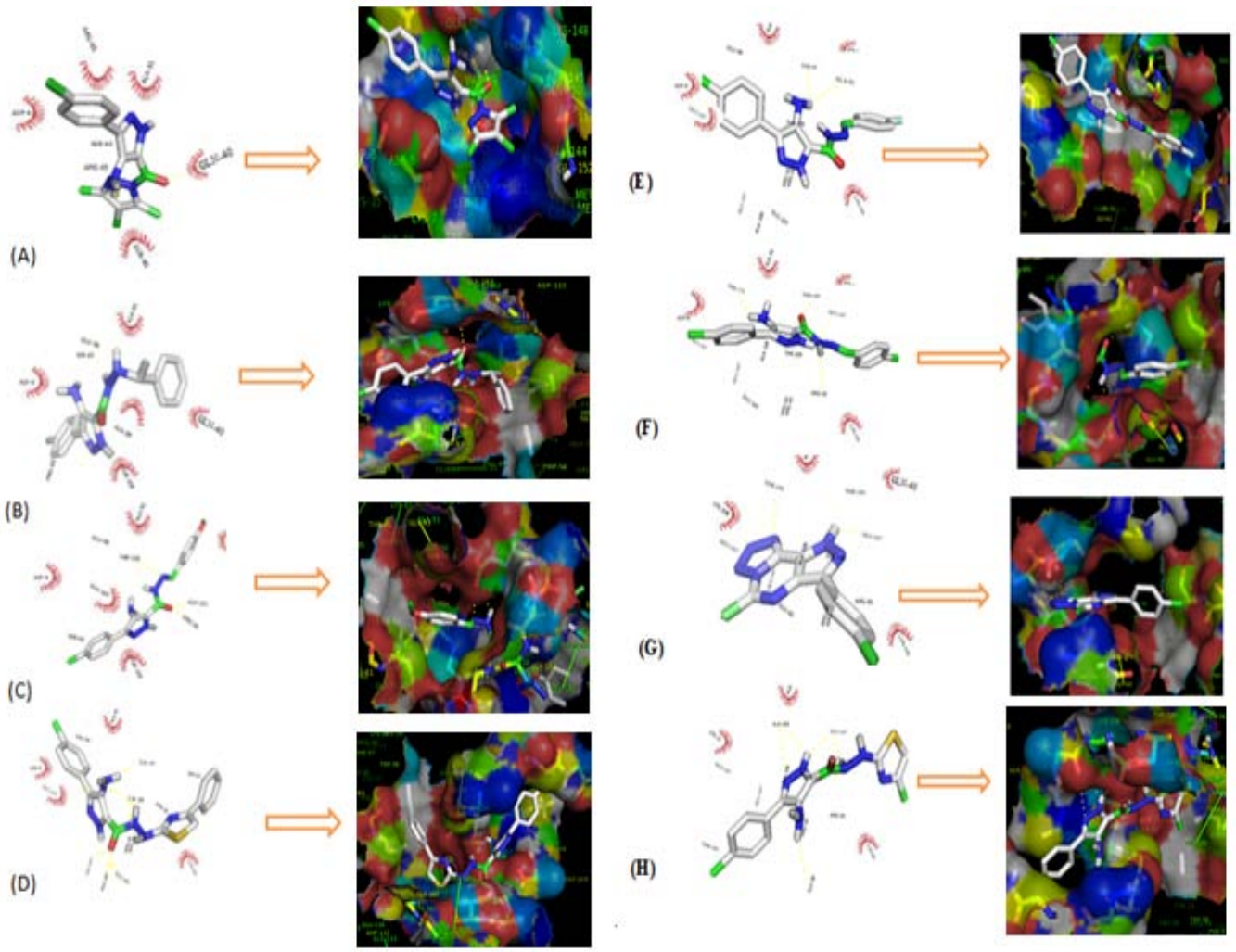

Figure 4: Binding interactions: (A) for 3b, (B) for 10a (C) for 10d and (D) for 19b (E) for 10b (F) for 10c (G) for 15 (H) for 19a with 2N8A

IV. Conclusion

In this study, the quantum chemical method via density functional theory (DFT) method was used for calculation of molecular descriptors relating to the anticancer activity of pyrazole derivatives. The QSAR analysis revealed the efficiency of the model developed using multiple linear regression (MLR), and that the QSAR model replicated the observed bioactivities of the studied compounds against colon cancer cells line (ID: 2N8A). Furthermore, the simulated molecular docking predicted stable conformations of the drug-like molecules (Pyrazolederiatives) in the active gouge of the receptor. Also, the binding energy as well as, nature of electrostatic interactions of the ligands in the ligand-receptor complexes were obtained for the twenty compounds.

References Références Referencias

1. Gamal El-Din MM, El-Gamal MI, Abdel-Maksoud MS, Yoo KH, Oh, CH. Design, synthesis, broad-spectrum antiproliferative activity, and kinase inhibitory effect of triarlpyazole derivatives possessing arylamides or arylureas moieties.Eur J Med Chem2016; 119: 122-131.
2. GibbsJB. Mechanism-based target dentification and drug discovery in cancer research. Science 2000; 287: 1969-1971.
3. PanteaP, RaviS, ElenaP. Influence of Far Infrared Radiation on cytotoxicity of Human Breast Cancer (MCF7) cells: experimental evaluation. IWBBIO Proceedings 2013.
4. JemalA. et.al. Global cancer statistics. AcanJ for clin2011; 61(2): 69-90.
5. HuertaS, Goulet EJ, Livingston EH. Colon cancer and apoptosis. Am J Surg2006; 191: 517-526.
6. INCA – Institutonacional de câncerAções de prevençãoprimáriaesecundária no controle do câncer. Rio de Janeiro: Inca 2008; 628.
7. SteinK, BorowickiA, ScharlauD, SchettlerA, ScheuK. et al. Effects of synbiotic fermentation products on

primary chemoprevention in human colon cells. JNutrBiochem2012; 23: 777-784.
8. GuL, WangP, ZhongQ, DengY, XieJ, LiuF, XiaoF, ZhengS, ChenY, WangGand HeL. Copper salt-catalyzed formation of a novel series of triazole–spirodienone conjugates with potent anticancer activity.RSC Adv2017; 7: 9412–9416.
9. Kumar KS, SastryN, PolakiH, MishraV. Colon Cancer Prevention through Probiotics: An Overview. J Cancer SciTher 2015; 7: 081-092. doi: 10.4172/1948-5956.1000329.
10. GursoyA, DemirayakS, CapanG, ErolK, VuralK. Synthesis and preliminary evaluation of new 5-pyrazolinone derivatives as analgesic agents.Eur J Med Chem2000; 35: 359-364.
11. Prakash O, KumarR, ParkashV, PrakashO, KumarR, ParkashV. Synthesis and antifungal activity of some new 3-hydroxy-2- (1-phenyl-3-aryl-4-pyrazolyl) chromones. Eur J Med Chem2008; 43: 435.
12. StorerR, Ashton CJ, Baxter AD, Hann MM, Marr CLP, Mason A M, Mo CL, Myers PL. Noble, S.A.; Penn, C.R, Weir, N.G.; Woods, J.M.; Coe, P.L., The synthesis and antiviral activity of 4-fluoro-1-beta-D-ribofuranosyl- 1H- pyrazole- 3- carboxamide. Nucleosides Nucleotides1999; 18: 203.
13. GeninMJ, Biles C, Keiser BJ, Poppe SM, Swaney SM, Tarpley WG, YagiY, Romero DL. Novel 1, 5-Diphenylpyrazole Nonnucleoside HIV-1 reverse transcriptase inhibitors with enhanced activity versus the delavirdine-resistant P236L mutant: Lead identification and SAR of 3- and 4-substituted derivatives.J Med Chem2000; 43(5): 1034-1040.
14. ChengH, DeMello KML, LiJ, Sakya SM, Ando K et al. Synthesis and SAR of heteroaryl-phenyl-substituted pyrazole derivatives as highly selective and potent canine COX-2 inhibitors. Bioorg Med ChemLett 2006; 16: 2076-2080.
15. Bekhit AA, Ashour HMA, Ghany YSA, Bekhit AEA, BarakaA. Synthesis and biological evaluation of some thiazolyl and thiadiazolyl derivatives of 1H-pyrazole as anti-inflammatory antimicrobial agents. Eur J Med Chem2008; 43:456-463.
16. El-Feky SA, Abd El- SamiiZK. Synthesis and antihypertensive activity of novel 1-(4-benzyl- 1-phthalazinyl)- pyrazolo [3,4-d] pyrimidines. Pharmazie1996; 51: 540-543.
17. KurodaS, AkahaneA, ItaniH, NishimuraS, durkinK, KinoshitaT, TendaY, SakaneK. Discovery of FR166124, a novel water-soluble pyrazolo-[1, 5-α] pridine adenosine A_1 receptor antagonist. Bioorg Med ChemLett1999; 9(14):1979-1984.
18. Moustafa MG, Zeinab HI, Soad MA, Anhar AA. Antimicrobial activity of amino acid, imidazole, and sulfonamide derivatives of pyrazolo [3,4-d]pyrimidine.HeteroatChem2004; 15(1): 57-62.
19. Lindell SD, Moloney BA, Hewitt BD, Earnhaw CG, Philip PJ, Dancer JE. The design and synthesis of inhiitors of adenosine 5`- monophosphate deaminase. Bioorg Med ChemLett1999; 9: 1985-1990.
20. Hend NH, El-Gazzar Abdel-Rhman BA, Al-Hussain Sami,A. Novel pyrazole derivatives with oxa/thiadiazolyl, pyrazolyl moieties and pyrazolo[4,3-d]-pyrimidine derivatives as potential antimicrobial and anticancer agents. Bioorganic & Medicinal Chemistry Lett2016. http://dx.doi.org/10.1016/j.bmcl.2016. 03.117
21. StehlikJ, Movsesian MA. Inhibitors of cyclic nucleotide phosphodiesterase 3 and 5 as therapeutic agents in hearts in heart failure. Expert Opin Invest Drugs2006; 15: 733-742.
22. PandeyaSNand RaiP. Review: Synthesis & Biological Activity of Benzimidazole Derivatives.J SciRes Phar2012; 1(4): 1-4.
23. Santosh PC, PandeyaSN, and Pathak AK. Benzimidazole: a versatile chemical entity. IJRAP2011; 2(6): 1726-1737.
24. HanschC. A quantitative approach to biochemical structure-activity relationships. Acc of Chem Res1969; 2: 232-239.
25. Ramsden CA. Quantitative Drug Design of comprehensive Medicinal Chemistry, Oxford. 1990; 4.
26. Dahl GE, JaitlyN, SalakhutdinovR. Multitask Neural Networks for QSAR Predictions. arXiv preprint arXiv.2014; 1231.
27. Oyebamiji AK, and SemireB. Studies of antihypertensive activity of 1, 4dihydropyridine derivatives: combinations of DFT-QSAR and docking approaches. Bulletin of Pharmaceutical Research2016; 6(3): 105-113.
28. OyebamijiKA, and SemireB. Studies of 1, 4-Dihydropyridine Derivatives for Anti-Breast Cancer (MCF-7) Activities: Combinations of DFT-QSAR and Docking Methods. New York Science Journal2016; 9(6):58-66.doi:10.7537/marsnys09061610.
29. Oyebamiji AK and SemireB.DFT-QSAR model and docking studies of anti liver cancer (HEPG-2) activities of 1, 4-diydropyridine based derivatives. Cancer Bio2016; 6(2): 69-72. doi:10.7537/marscbj06021610.
30. Arulmozhiraja S, Morita M. Structure-activity relationships for the toxicity of polychhorinated-dibenzofurans: approach through density functional theory-based descriptors. Chem ResToxicol2004; 17: 348-356.
31. Gu C, JiangX, Ju XH, YangXL, Bian YR, SunC. QSARs for congener-specific toxicity of polyhalogenateddibenzo-p-dioxins with DFT and WHIM theory. Ecotoxicol EnvironSaf 2009; 72: 60-70.
32. ErogluE, and TurkmenH. A DFT-based quantum theoretic QSAR study of aromatic and heterocyclic sulfonamides as carbominc anhydrase inhibitors

against isozymeCA-II. J. Mol. Graph.Model 2007; 26: 701-708.
33. ZhuM, GeF, ZhuR, WangX, and ZhengX. A DFT-based QSAR study of the toxicity of quaternary ammonium compounds on Chlorella vulgaris. Chemosphere2010; 80: 46-52.
34. Jain A.N. Scoring functions for protein-ligand docking. Current Protein Peptide science. 2006; 7(5): 407-420.
35. Taylor RD, Jewsbury PJ, Essex JW. A review of protein-small molecule docking methods. Journal of Computer-Aided Molecular Design. 2002;16: 151-166.
36. BeckeAD. Density functional thermo chemistry. III. The role of exact exchange. Jof phy Chem1993; 98: 5648 – 5652.
37. LeeC, YangW & Parr RG. Development of the Colle-Salvetti correlation-energy formula into a functional of the electron density. Phys Rev B1988; 37: 785-789.
38. JacqueminD, PerpeteEA, CiofiniI, AdamoC. Accurate simulation of optical properties in dyes. Acc of chem Res2008; 42: 326 – 3344.
39. Spartan 14 wave function Inc. Irvine, CA 92612, USA.
40. GoodarziM, Dejaegher B, Vander HeydenY. Features selection methods in QSAR studies.J AOACInt2012: 95(3): 636-51.
41. EustermannS, Wu WF, Langelier MF, Yang JC, Easton LE, Riccio AA, Pascal JM and NeuhausD. Structural Basis of Detection and Signaling of DNA Single-Strand Breaks by Human PARP-1.Molecular Cell2015; 60: 742–754.
42. SapnaR, Ajeet Arvind K. Designing of Sulfanilamide/ Sulfacetamide Derivatives as Human Topoisomerase II Inhibitor: A Docking Approach. Ame J of Pharm Sci2014: 2(2); 42-46.
43. ChiricoN, and GramaticaP. Real external predictivity of QSAR models: How to evaluate it? Comparison of Different validation criteria and proposal of using the concordance correlation coefficients. J ChemInf Model2011; 51(9): 2320-2335.
44. Chirico N, and Gramatica P. Real external predictivity of QSAR models. Part 2. New inter-comparable thresholds for different validation criteria and the need for scatter plot inspection. J Chem Inf Model2012; 52(8): 2044-2058.
45. Marrero PY, Castillo GJA, TorrensF, Romero ZV, and Castro EA. Atom, atom-type, and total linear indices of the molecular pseudograph's atom adjacency matrix": application to QSPR/QSAR studies of organic compounds. Molecules 2004; 9(12): 1100–1123.
46. ParamitaRI, ArsiantiA, RadjiM. In Silico Docking Studies of Alkyl Esters Derivative of Gallic Acid on Bcl-xL Anti-apoptotic Protein of Breast Cancer. International Journal of Chem Tech Res2017; 10(1): 348-355.
47. AdejoroIA, Waheed SO, Adeboye OO. Molecular Docking Studies of *Lonchocarpuscyanescens* Triterpenoids as Inhibitors for Malaria. J Phys ChemBiophys 2016; 6: 213. doi:10.4172/2161-0398.1000213.